Meteorol Atmos Phys
DOI 10.1007/s00703-008-0007-2

ORIGINAL PAPER

# A study of the microphysical processes in a numerically simulated heavy snowfall event in North China: the sensitivity of different snow intercept parameters

**Wenshi Lin · Jinping Meng · C.-H. Sui · Weiguang Meng · Jiangnan Li**

Received: 25 September 2007 / Accepted: 16 October 2008


**Abstract** We performed a modeling study of the cloud processes in a heavy snowfall event occurring in North China on 20–22 December 2004. The nonhydrostatic Mesoscale Model (MM5) was used to carry out experiments with the Reisner-2 explicit microphysical parameterizations in four nested domains to test the sensitivity of simulated heavy snowfall to different snow intercept parameters. Results show that while the different intercept parameters do not significantly affect the accumulated snowfall amounts at the surface in either total amount or location, some microphysical characteristics of the modeled heavy snowfall event are impacted. The budget of cloud microphysics is analyzed to determine the dominant cloud processes. In the control experiment (CTL) with the snow intercept ($N_{os}$) specified as a function of temperature, the primary simulated hydrometeor is snow, and its mixing ratio is an order of magnitude larger than that of the other cloud species. Relative to CTL, the experiment with a fixed intercept (CON3E6) produced lower snow mixing ratios, more cloud water and graupel mixing ratios. Among the two experiments, while snowfall is slightly smaller in CON3E6, other processes like the rate of graupel fall, condensation and evaporation of cloud water, deposition and sublimation of graupel are all larger in CON3E6 than in CTL. Among CTL, CON3E6, and two more experiments (CON2E7: with a smaller fixed intercept; and NOSQS: $N_{os}$ a function of snow mass mixing ratio), the budget shows that CON3E6 produces the smallest deposition and sublimation of snow, the largest deposition of cloud ice, and the largest conversion from cloud ice to snow.

W. Lin (✉) · J. Li
School of Environmental Science and Engineering,
Sun Yat-sen University, 510275 Guangzhou,
People's Republic of China
e-mail: eeslws@mail.sysu.edu.cn

J. Meng
Beijing Meteorological Bureau, 100089 Beijing,
People's Republic of China

C.-H. Sui
Institute of Hydrological and Oceanic Sciences,
National Central University, Jhongli 32001, Taiwan

W. Meng
Institute of Tropical and Marine Meteorology,
China Meteorological Administration,
510080 Guangzhou, People's Republic of China

## 1 Introduction

Extremely heavy snowfall is a primary weather disaster in Northern China. The Chinese Meteorological Administration (CMA) defines "heavy snowfall" as those events with a daily snowfall exceeding 10 mm. In recent years, heavy snowfalls frequently occurred in XinJiang, Inner Mongolia, and the eastern end of the Tibetan Plateau. They caused a large number of domestic animals in pasturing areas to be frozen to death. The traffic in the area was congested, and the economics were depressed by these events. It is imperative to better understand the evolution and structure of heavy snowfall, in order to improve their parameterization in numerical models for predicting snowfall.

Cloud models have been used extensively in the study of microphysical process of hailstorms or tropical convection (Kong et al. 1991; Hong et al. 2002; Tao et al. 2003; Grabowski 1998; Li et al. 1999; Sui et al. 1998). Because heavy snowfall is different from thunderstorms and hailstorms, the simple cloud model cannot be used to run an

idealized simulation of heavy snowfall. Heavy snowfall typically requires a larger-scale model for proper simulation, including the incorporation of time-dependent lateral boundary conditions and synoptic-scale forcing (Reisner et al. 1998).

Recently, the adequate representation of cloud physics' processes became one of the most challenging tasks in the numerical simulation and prediction of mesoscale systems. One may divide the treatments of cloud processes in a mesoscale model into two categories: the cumulus parameterization (implicit) and the parameterization of cloud microphysical process (explicit) where the implicit scheme is used to remove the convective instability and the explicit scheme is used to treat the cloud precipitation processes on convective stability and the nearly neutral layer (Zhang 1998; Molinari and Dudek 1992). When grid sizes are smaller than 5 km, only the parameterization of the microphysical process is generally used because the cumulus can be resolved (Weisman et al. 1997).

Based on the above motivations, we conducted systematic modeling studies about the influence of cloud microphysics on heavy snowfall events, using the fifth-generation Pennsylvania State University-National Center for Atmospheric Research (PSU-NCAR) nonhydrostatic Mesoscale Model (MM5; Dudhia 1993; Grell et al. 1994). First, Lin et al. (2007) conducted a numerical comparison study of the dominant cloud microphysical processes in a simulated heavy snowfall event by the Goddard cloud microphysics scheme (Tao and Simpson 1993; modified by Braun and Tao 2000) and the Reisner-2 cloud microphysics scheme (Reisner et al. 1998; modified by Thompson et al. 2004). In the current study, we further examine the simulated ice clouds in a heavy snowfall event and associated ice cloud microphysics parameterization in the Reisner-2 scheme.

The paper contains the following sections. In Sect. 2, we give an overview of the heavy snowfall event in North China. Section 3 contains descriptions of the data source, the numerical model setup, the design of sensitivity experiments with respect to different cloud snow intercept parameters in the Reisner-2 scheme, and the analysis methods. In Sect. 4, the numerical simulation results are presented in which the sensitivities of snow intercept parameters and their budgets are included. The results and implications are discussed in Sect. 5.

## 2 Overview of the synoptic weather

An anti-cyclone existed near Lake Baikal from 0000UTC 20 December to 0000UTC 21 December 2004 (Zhang 2005). A cold trough moved eastward to the eastern part of southwest China and the western part of south China, and the associated cold air moved eastward and southward. Meanwhile, a low pressure existed in southwest China, and a trough formed in northwest China at 0000UTC 21 December 2004 (Fig. 1a). Subsequently, the trough strengthened (Fig. 1b). A warm, moist, tropical air mass collided with a cold, polar air mass, triggering moderate winter rainfall and heavy snowfall in the greater part of North China (Fig. 2a).

Figure 3 shows the sign of 700 hPa horizontal advection of water vapor and wind fields calculated from the $1^\circ \times 1^\circ$ resolution global reanalysis data from the National Center for Environmental Prediction (NCEP) (Kistler et al. 2001). The positive horizontal advection region of water vapor is located in the region of North China. Before the rainfall and snowfall, south westerlies prevailed and provided uninterrupted warm, moist air. As a result, a heavy snowfall occurred in the valley of the Yellow River and a moderate rainfall in the middle and lower reaches of the Yangtze River. From Fig. 2b, in this event, the maximum total snowfall from 0000UTC 21 to 0000UTC 22 December 2004, was 15 mm, measured by a rain gauge at Shijiazhuang Observation Station in Hebei province (38°N, 114.5°E). It was the greatest single-event snowfall amount and reached the level of heavy snowfall. There were also moderate and heavy snowfalls near North China.

## 3 Model and experiment design

MM5 version 3.7 was used to simulate the heavy snowfall event from 1200UTC 20 December to 0000UTC 22 December 2004 in North China. The model domain includes four nested domains, as shown in Fig. 4. On a Lambert conformal map, the coarse domain (D01) covers $88 \times 97$ grid points with the grid length of 54 km. The central latitude and longitude are 36°N and 110°E, respectively. The domain D02 has $97 \times 97$ grid points with the grid length of 18 km; the domain D03 has $79 \times 79$ grid points with the grid length of 6 km; the domain D04 has $49 \times 49$ grid points with the grid length of 2 km. Domains D02, D03, and D04 are two-way nested within D01. Vertically, from the top to surface level, 24 levels (i.e., 23 sigma levels) are used for MM5 ($\sigma = 0.00$, 0.05, 0.10, 0.15, 0.20, 0.25, 0.30, 0.35, 0.40, 0.45, 0.50, 0.55, 0.60, 0.65, 0.70, 0.75, 0.80, 0.85, 0.89, 0.93, 0.96, 0.98, 0.99, 1.00), with $\sigma = 1.0$ corresponding to the bottom of the atmosphere. The model top is 50 hPa.

The initial and boundary conditions (atmospheric variables, and soil moisture and temperature) are derived from the 6-hourly NCEP global reanalysis data at $1^\circ \times 1^\circ$ grid resolution (Kistler et al. 2001). The NCEP data are interpolated to the $88 \times 97$ coarse model grids (resolution at 54 km) at 23 sigma levels. Surface and upper-air conventional observation data were incorporated into the analysis

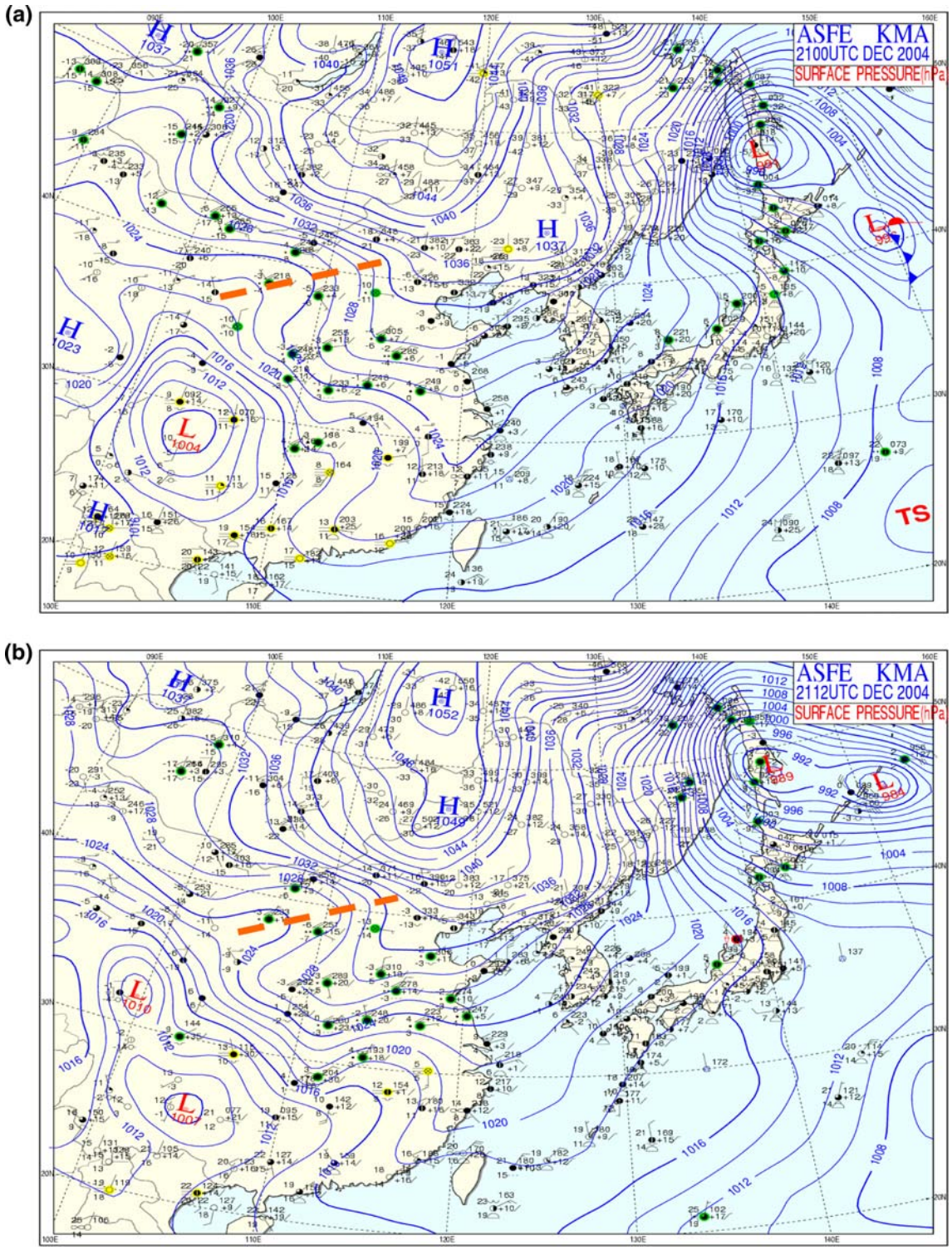


**Fig. 1** Surface analysis at **a** 0000UTC 21 December 2004 and **b** 1200UTC 21 December 2004. Figures were downloaded from the web of the Korea Meteorological Administration

using a Cressman-type analysis scheme (Benjamin and Seaman 1985). Initial conditions for the three finer domains were obtained by interpolation from the coarsest domain. In order to reduce the initial imbalance of the model, the integrated mean divergence in a column is removed at all times as well. The upper radiative boundary condition was applied in order to prevent gravity waves from being reflected off the model top (Klemp and Durran 1983).

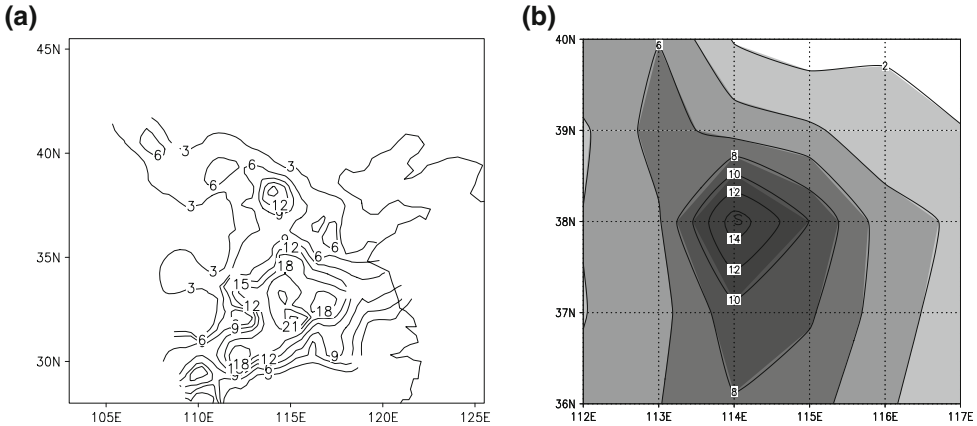


**Fig. 2** The observed 24-h accumulated precipitation (in units of mm) from 0000 UTC 21 December 2004 to 0000 UTC 22 December 2004, over North China, within **a** the domain D02 and **b** the domain D03 of Fig. 4. Contour interval is 3 mm in **a** and 2 mm in **b**

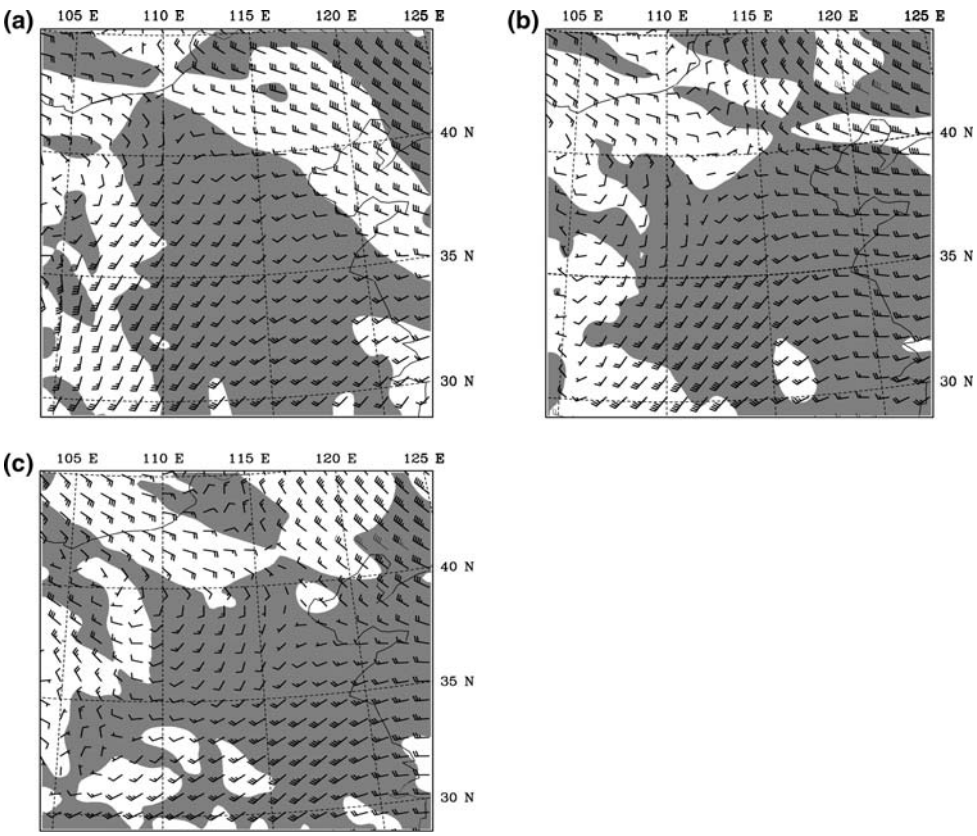


**Fig. 3** Horizontal wind vectors (full barb, 5 m $s^{-1}$) and horizontal advection of water vapor at 700 hPa from the NCEP reanalysis data at **a** 1200UTC 20 December 2004, **b** 0000UTC 21 December 2004, and **c** 1200UTC 21 December 2004. *Shaded* denotes the positive horizontal advection region of water vapor

Topography was taken from the United States Geological Survey (USGS) 5-min resolution data set and interpolated onto the model grid using a Cressman type objective analysis scheme. The 25-category USGS land use classification scheme was adopted to provide land-cover data for the model domains.

The model physics in all simulated domains consist of the medium-range forecast (MRF) planetary boundary layer scheme (Hong and Pan 1996), five-layer simple soil model (Dudhia 1996), NCAR Community Climate Model (CCM2) longwave and shortwave schemes (Hack et al. 1993), and the surface energy budget for calculating the ground temperature. In addition, the Grell cumulus parameterization scheme (Grell et al. 1994) is used for the two outermost domains (D01 and D02), whereas for the other two inner domains (D03 and D04) convection is assumed to be resolved reasonably well by the explicit microphysical parameterization scheme, and no cumulus parameterization scheme is used (Weisman et al. 1997). All simulations used the Reisner-2 explicit moisture scheme (Reisner et al. 1998), with further modifications by Thompson et al. (2004), in all simulated domains.

A set of experiments was completed using different microphysical parameters within the Reisner-2 scheme in

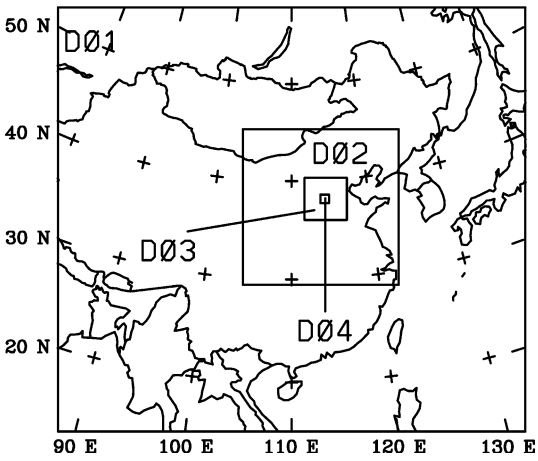


**Fig. 4** Nested domains used for MM5 simulations: D01 54-km grid spacing, D02 18-km grid spacing, D03 6-km grid spacing, D04 2-km grid spacing

**Table 1** List of microphysical sensitivity experiments completed for MM5

| Experiment name | Description |
|---|---|
| CTL | Reisner-2, $N_{OS}(T)$ |
| CON2E7 | Reisner-2, fixed $N_{os}$, $N_{OS} = 2 \times 10^7$ m$^{-4}$ |
| CON3E6 | Reisner-2, fixed $N_{os}$, $N_{OS} = 3 \times 10^6$ m$^{-4}$ |
| NOSQS | Reisner-2, $N_{os}(q_s)$ |

order to quantify sensitivities for the heavy snowfall in North China. The model setups of different experiments are the same except for different snow intercept parameters. The parameters for these sensitivity experiments are listed in Table 1. The goal of these sensitivity simulations is not to find a fix to the Reisner-2 microphysical parameterization, but to focus primarily on those processes that are important to snow growth. CTL exploited the Reisner-2 ice phase microphysical scheme, in which the snow intercept parameter (Nos) is a function of temperature (Thompson et al. 2004):

$$N_{OS}(T) = \min\{2 \times 10^8, 2 \times 10^6 \times \exp[-0.12 \min(-0.001, T - T_0)]\}$$

where $T_0 = 273.15$ K. CON2E7 and CON3E6 used fixed snow intercept parameters $N_{OS} = 2 \times 10^7$ m$^{-4}$ and $N_{OS} = 3 \times 10^6$ m$^{-4}$, individually. NOSQS specified the snow intercept parameter as a function of the snow mixing ratio as described in Sekhon and Srivastiva (1970) and Reisner et al. (1998):

$$N_{os}(q_s) = \max\left\langle 2 \times 10^7, \left\{ 1.718 \left[ \frac{1}{\rho q_s \alpha} \left( \frac{\pi \rho_s}{\rho q_s} \right)^{\frac{b_s}{4}} \right]^{0.94} \right\}^{\frac{4}{4-0.94 b_s}} \right\rangle$$

where $1/\alpha = 6\rho_w / a_s \Gamma(4 + b_s)$, $\rho$ is the density of the air, $\rho_s$ is the density of the snow (100 kg m$^{-3}$), and $\rho_w$ is the density of the water (1000 kg m$^{-3}$), $a_s = 11.72\,\mathrm{m}^{1-b_s}\mathrm{s}^{-1}$, $b_s = 0.41$.

In order to determine which microphysical processes contributed most to the production and depletion of a specific hydrometeor category, the vertically integrated hydrometeor conversion rate $\bar{P}_q$ is used for a model microphysical budget. It is calculated:

$$\bar{P}_q = \sum_{i,j,k} p^*(i,j) \times P_q(i,j,k) \times \Delta\sigma(k)$$

where $p^*$ is the pressure difference between the surface and model top, $P_q(i, j, k)$ is the conversion rate of a specific microphysical process averaged for the two adjacent sigma levels, and $\Delta\sigma$ is the sigma level difference. In this study,

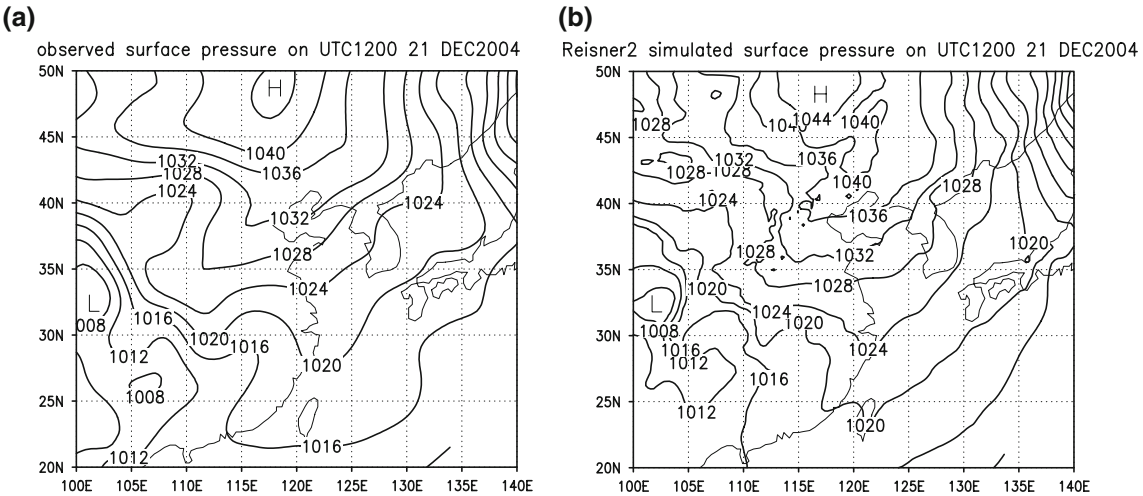


**Fig. 5** Sea level pressure (hPa) of **a** NCEP reanalysis and **b** CTL at 1200UTC 21 December 2004

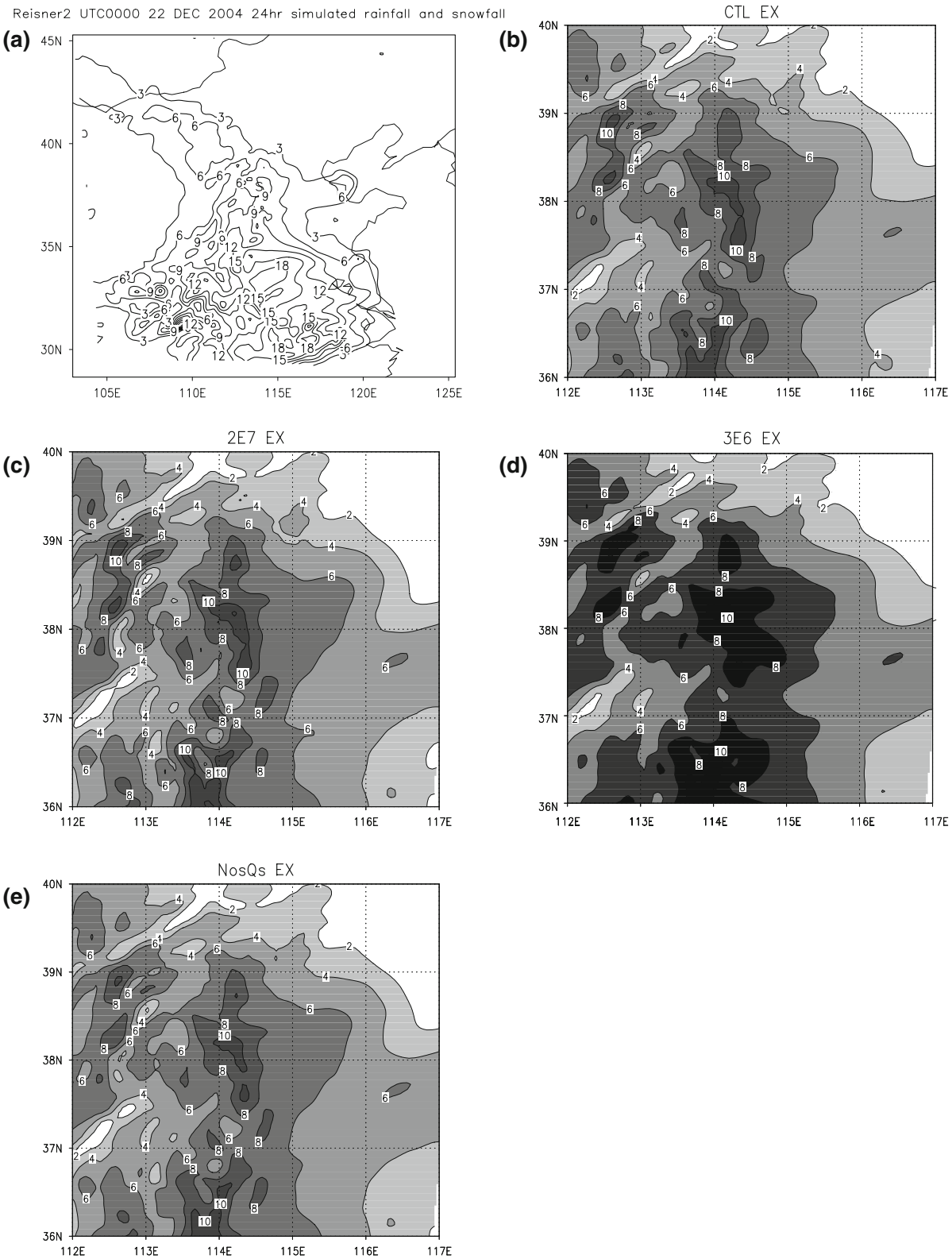


**Fig. 6** The 24-h accumulated precipitation (in units of mm) from 0000 UTC 21 December 2004 to 0000 UTC 22 December 2004 for **a** the CTL experiment in the domain D02, **b** the CTL experiment in the domain D03, **c** the CON2E7 experiment in the domain D03, **d** the CON3E6 experiment in the domain D03, and **e** the NosQs experiment in the domain D03. Contour interval is 2 mm

the vertically integrated hydrometeor conversion rate for each term in the prognostic equations of each hydrometeor species in the Reisner-2 scheme (Colle and Zeng 2004) was output every 1 h. Its unit is mm.

All four experiments were initialized at 1200UTC 20 December 2004 and integrated for 36 h. The time steps are 120, 40, 13.3, and 4.4 s for the domains D01, D02, D03, and D04, respectively.

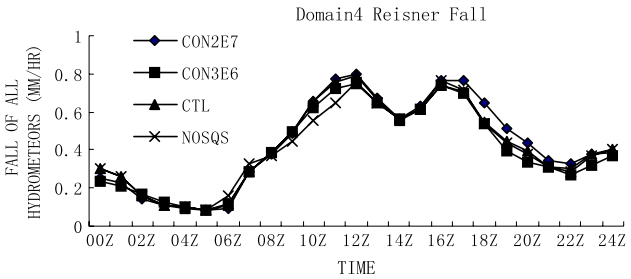


**Fig. 7** Domain-averaged precipitation rate (mm $h^{-1}$) for all four experiments in the domain D04

## 4 Results and discussion of the numerical simulations

### 4.1 Validation of synoptic scale and precipitation feature in the control experiment

Figure 5 shows the sea level pressure of the NCEP reanalysis and the simulation of the control experiment (CTL) at 1200 UTC 21 December 2004. The main characteristics of the sea level pressure are successfully simulated by CTL, except that the high pressure near Lake Baikal and the low pressure to the east of the Tibetan Plateau are over-predicted.

The CTL results of domain D02 in Fig. 6a show that 24-h simulated precipitation patterns capture the event well, which included the snowfall occurring in the valley of the Yellow River and rainfall in the middle and lower reaches of the Yangtze River (compared with Fig. 2a). Figure 6a shows that the maximum simulated snowfall of 12 mm occurred near 38°N, 114.5°E in Hebei province, which is coincident with the recorded snowfall of 15 mm at Shijiazhuang station.

The observed (Fig. 2b) and CTL results (Fig. 6b) in domain D03 also agree very well. There are many centers of simulated maximum precipitation amount in domain D03 because the horizontal model resolution of 6 km in the domain D03 can resolve some small clouds and their snowfall.

### 4.2 The comparison of snowfall pattern and hydrometeor distribution

The simulated precipitation in CON2E7, CON3E6, and NOSQS accumulated from 0000UTC 21 December 2004 to 0000UTC 22 December 2004 is shown in Fig. 6b–e. They all compare favorably with the observed precipitation (Fig. 2b) in terms of distribution and intensity, except that all simulated maxima of precipitation are slightly smaller than the observed. Meanwhile, there are many small snowfall centers, and some discrepancies also exist among all of the experiments. The surface precipitation patterns show that there is no obvious difference in the overall simulated snowfall distributions, and the major differences among the different experiments are located in the simulated snowfall centers, in which the values and positions are slightly different. Furthermore, the temporal evolution of domain averaged precipitation (Fig. 7) is quite similar among the four experiments.

Figure 8 shows the vertical distribution of domain (D04) and time (12–18 h) averaged hydrometeors in the four experiments. The figure shows that snow is the most dominant species with values of maximum mixing ratio around 0.12 g $kg^{-1}$ in the lower troposphere. Cloud ice is the second important species with peak values of 0.012 g $kg^{-1}$ centered within 6–10 km. Cloud water and graupel are two minor species in the simulations, except for the CON3E6 simulation where cloud water is of the same magnitude as cloud ice for all experiments. For mixing ratio and number concentration of cloud ice, there is no distinct difference among the four experiments. For the snow mixing ratio, there is more in CON2E7 and fewer in CON3E6. For the cloud water and graupel mixing ratio, values for the mixing ratio in CON3E6 are significantly large than those in the other three experiments. Moreover, there is a lesser cloud water mixing ratio in CON2E7 ($N_{OS} = 2 \times 10^7$ $m^{-4}$) than in CON3E6 ($N_{OS} = 3 \times 10^6$ $m^{-4}$), indicating that larger intercept would lead to less supercooled liquid water.

### 4.3 The domain-averaged budgets of microphysical process

There are 44 microphysical processes in the Reisner-2 scheme (see in Appendix of Colle et al. 2005). However, only 12 of them are active in this heavy snowfall in North China according to four sensitivity experiments. The dominant microphysical processes in this heavy snowfall are deposition of snow, sublimation of snow, deposition of graupel, sublimation of cloud ice, deposition of cloud ice, and conversion of cloud ice to snow. The condensation of cloud water, evaporation of cloud water, sublimation of graupel, collection of cloud water by snow, accretion of cloud ice by snow, and initiation of cloud ice are very small. Their domain-averaged (horizontally) and vertically integrated budgets within D04 for CTL and the other three experiments are shown in Table 2.

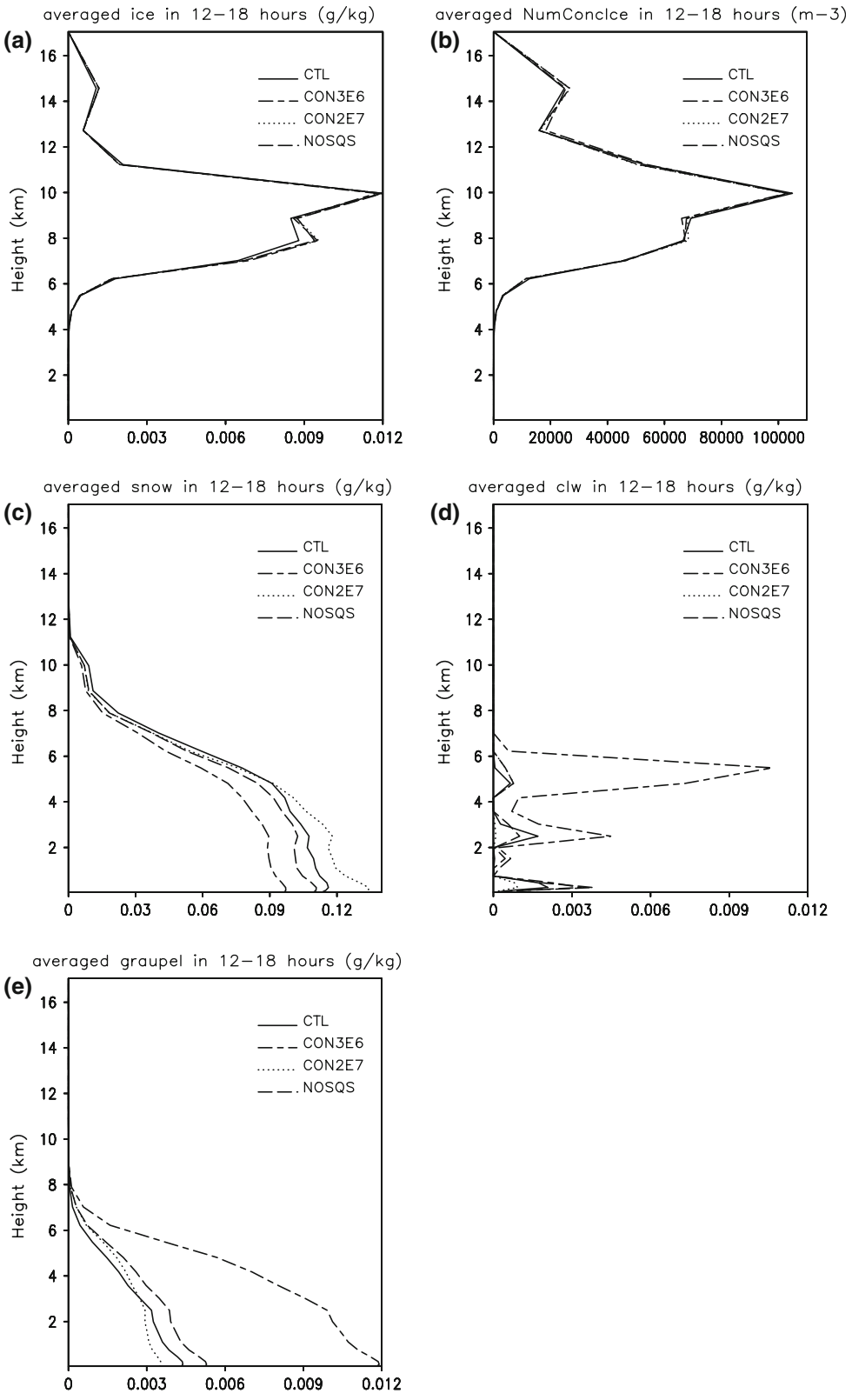


**Fig. 8** The domain-averaged hydrometeors depicted as a function of height in 12–18 h in four experiments in the simulated domain D04. **a** The cloud ice mixing ratio, **b** the number concentration of cloud ice, **c** the snow mixing ratio, **d** the cloud water mixing ratio, **e** the graupel mixing ratio. The units of mixing ratio and number concentration are g $kg^{-1}$ and $m^{-3}$, respectively. The units in the figures are normalized with respect to the number of horizontal model grid points

From Table 2a, the condensation rate of cloud water in CON3E6 (0.0113 mm $h^{-1}$) is one magnitude order greater than the three other experiments in 06–12 h. For the evaporation rate of cloud water, CON3E6 (0.0046 mm $h^{-1}$) has twice the rate of the three other experiments in 06–12 h. In 12–18 h, the condensation and

**Table 2** The domain averaged (horizontally) and vertically integrated cloud microphysics budgets within D04 and temporally averaged over (a) 06–12 h and (b) 12–24 h on 21 December 2004

| | Description | CTL | CON2E7 | CON3E6 | NOSQS |
|---|---|---|---|---|---|
| (a) 06–12 h | | | | | |
| Fall | Fallout of all hydrometeors | 0.4386 | 0.4390 | 0.4396 | 0.4275 |
| Fgraupel | Fallout of graupel | 0.0224 | 0.0171 | 0.0697 | 0.0254 |
| Fsnow | Snowfall | 0.4162 | 0.4219 | 0.3699 | 0.4022 |
| Cond | Condensation of cloud water | 0.0030 | 0.0012 | 0.0113 | 0.0031 |
| Evap | Evaporation of cloud water | 0.0026 | 0.0020 | 0.0046 | 0.0024 |
| Pgdep | Deposition of graupel | 0.0245 | 0.0187 | 0.0748 | 0.0283 |
| Pgsub | Sublimation of graupel | 0.0017 | 0.0012 | 0.0030 | 0.0016 |
| Psdep | Deposition of snow | 0.4952 | 0.4732 | 0.4178 | 0.4348 |
| Pssub | Sublimation of snow | 0.0322 | 0.0430 | 0.0187 | 0.0381 |
| Pidep | Deposition of cloud ice | 0.0823 | 0.0971 | 0.1210 | 0.0840 |
| Pisub | Sublimation of cloud ice | 0.0047 | 0.0059 | 0.0056 | 0.0059 |
| Pidsn | Initiation of cloud ice | 0.0006 | 0.0007 | 0.0008 | 0.0007 |
| Psacw | Collection of cloud water by snow | 0.0002 | 0.0000 | 0.0048 | 0.0002 |
| Pscni | Conversion from cloud ice to snow | 0.0654 | 0.0820 | 0.1037 | 0.0825 |
| Psaci | Accretion of cloud ice by snow | 0.0002 | 0.0001 | 0.0000 | 0.0015 |
| (b) 12–18 h | | | | | |
| Fall | Fallout of all hydrometeors | 0.6738 | 0.6851 | 0.6736 | 0.6547 |
| Fgraupel | Fallout of graupel | 0.0249 | 0.0223 | 0.0840 | 0.0388 |
| Fsnow | Snowfall | 0.6489 | 0.6628 | 0.5896 | 0.6159 |
| Cond | Condensation of cloud water | 0.0001 | 0.0000 | 0.0058 | 0.0010 |
| Evap | Evaporation of cloud water | 0.0003 | 0.0000 | 0.0112 | 0.0112 |
| Pgdep | Deposition of graupel | 0.0227 | 0.0202 | 0.0759 | 0.0346 |
| Pgsub | Sublimation of graupel | 0.0005 | 0.0006 | 0.0011 | 0.0006 |
| Psdep | Deposition of snow | 0.5122 | 0.5167 | 0.4036 | 0.4771 |
| Pssub | Sublimation of snow | 0.0219 | 0.0179 | 0.0076 | 0.0119 |
| Pidep | Deposition of cloud ice | 0.0635 | 0.0794 | 0.1091 | 0.0760 |
| Pisub | Sublimation of cloud ice | 0.0048 | 0.0054 | 0.0059 | 0.0055 |
| Pidsn | Initiation of cloud ice | 0.0005 | 0.0006 | 0.0007 | 0.0006 |
| Psacw | Collection of cloud water by snow | 0.0000 | 0.0001 | 0.0006 | 0.0001 |
| Pscni | Conversion from cloud ice to snow | 0.0511 | 0.0677 | 0.0968 | 0.0685 |
| Psaci | Accretion of cloud ice by snow | 0.0003 | 0.0002 | 0.0001 | 0.0013 |

Unit: mm $h^{-1}$

evaporation rate of CTL and CON2E7 are very small (Table 2b).

In response to the smaller fixed intercept ($N_{OS} = 3 \times 10^6$ $m^{-4}$) in CON3E6 relative to $N_{OS}$ in the other three experiments, the following features of CON3E6 are noted: the deposition and sublimation of graupel and deposition of cloud ice are the largest, while the deposition and sublimation of snow are smallest in all four experiments. But there is no obvious difference in the sublimation of cloud ice among all experiments.

Among the four sensitivity experiments, the conversion from cloud ice to snow in CON3E6 is the largest, and the conversion in CTL is the smallest. The initiation of cloud ice, the collection of cloud water by snow, and the accretion of cloud ice by snow in all experiments are very small and negligible.

While the falling rate of the solid hydrometeors (snow and graupel) among the four experiments do not seem to differ significantly, we still note some differences in Table 2. For the small fixed intercept ($N_{OS} = 3 \times 10^6$ $m^{-4}$) in CON3E6, the snowfall is slightly smaller (during 06–12 h, 0.3699 mm $h^{-1}$; during 12–18 h, 0.5896 mm $h^{-1}$) and the fall of graupel is slightly larger (during 06–12 h, 0.0697 mm $h^{-1}$; during 12–18 h, 0.0840 mm $h^{-1}$) than those in the other three experiments.

To sum up the features of the microphysics budget of CON3E6 compared with that of the other three experiments, the condensation, evaporation, deposition, and

sublimation of graupel, and deposition of cloud ice are larger, while the deposition and sublimation of snow are smaller, the snowfall is slightly smaller, and the falls of graupel are slightly larger. This may be a result of less snow, but more cloud water and graupel in CON3E6.

## 5 Summary

We perform a set of numerical experiments to simulate a heavy snowfall case in Northern China using the PSU-NCAR MM5V3 nonhydrostatic dynamical mesoscale model. The goal of the study is to investigate the impacts of microphysical parameters in the Resner-2 cloud microphysics scheme. Four experiments were designed to test the sensitivity of simulated surface precipitation, mixing ratio, and bulk microphysical processes to fixed or variable intercepts for the number concentration of snow.

Although Woods et al. (2007) show that changes in both the mass–diameter and velocity–diameter relationships significantly redistribute precipitation, the numerical results of this study indicate that variations in the snow intercept parameter do not alter the snowfall horizontal distribution/patterns, but significantly change the vertical distribution of hydrometeors and some microphysical processes. The dominant microphysical processes in this heavy snowfall are deposition of snow, sublimation of snow, deposition of graupel, sublimation of cloud ice, deposition of cloud ice, and conversion of cloud ice to snow. The condensation of cloud water, evaporation of cloud water, sublimation of graupel, collection of cloud water by snow, accretion of cloud ice by snow, and initiation of cloud ice are relatively small.

The Resner-2 cloud microphysics scheme produces a smaller snow mixing ratio, greater cloud water mixing ratio, and a greater graupel mixing ratio when using the small fixed intercept (CON3E6). The relative effect of small fixed intercept on the cloud microphysical processes is further investigated through an analyzed of vertically integrated microphysics budgets. The budgets of CON3E6 relative to the budgets of the other three experiments show the following features: the snowfall is slightly smaller, the fall of graupel is slightly larger, the condensation and evaporation rates of cloud water are the largest, the deposition and sublimation of graupel are the largest, its deposition and sublimation of snow are the smallest, the deposition of cloud ice is the largest, and the conversion from cloud ice to snow is the largest of the four experiments.

The goal of this paper is not to search ways to modify the cloud microphysics scheme, but to examine the sensitivity of the simulations to the snow intercept, which is important to snow growth. The results indicate that the tested microphysical parameters do not affect the heavy snowfall very much, but they do affect microphysical characteristics significantly. Overall, this study has improved our understanding of the complex bulk microphysical scheme for winter precipitation. We need more high-resolution, three-dimensional simulations and more observations to systematically evaluate microphysical schemes, particularly for solid precipitation.

**Acknowledgments** This research was supported by the National Natural Science Foundation of China (grant no. 40375036). The comments of two anonymous reviewers are acknowledged.

## References

Benjamin SG, Seaman NL (1985) A simple scheme for objective analysis in curved flow. Mon Wea Rev 113:1184–1198

Braun SA, Tao WK (2000) Sensitivity of high-resolution simulations of Hurricane Bob (1991) to planetary boundary layer parameterizations. Mon Weather Rev 128:3941–3961

Colle BA, Zeng Y (2004) Bulk microphysical sensitivities within the MM5 for orographic precipitation. Part I: the Sierra 1986 event. Mon Wea Rev 132:2780–2801

Colle BA, Garvert MF, Wolfe JB, Mass CF, Woods CP (2005) The 13–14 December 2001 IMPROVE-2 event. Part III: simulated microphysical budgets and sensitivity studies. J Atmos Sci 62:3535–3558

Dudhia J (1993) A non-hydrostatic version of the Penn State-NCAR mesoscale model: validation tests and simulations of an Atlantic cyclone and cold front. Mon Wea Rev 121:1493–1513

Dudhia J (1996) A Multi-layer soil temperature model For MM5. Preprint from the sixth PSU/NCAR mesoscale model users' workshop, Bouilder (http://www.mmm.ucar.edu/mm5/lsm/lsm-docs.html)

Grabowski WW (1998) Toward cloud resolving modeling of large-scale tropical circulations: a simple cloud microphysics parameterization. J Atmos Sci 55:3283–3298

Grell GA, Dudhia J, Stauffer DR (1994) A description of the fifth-generation Penn State/NCAR mesoscale model (MM5). NCAR technical note, NACR/TN-398+STR, National Center for Atmospheric Research, Boulder, 117 pp

Hack JJ, Boville BP, Kiehl JT, Rasch PJ, Williamson DL (1993) Description of the NCAR community climate model (CCM2), NCAR technical note, NCAR/TN-382+STR, National Center for Atmospheric Research, Boulder, 108 pp

Hong FY, Pan HL (1996) Nonlocal boundary layer vertical diffusion in a medium-range forecast model. Mon Wea Rev 124:2322–2339

Hong YC, Xiao H, Li HY, Hu ZX (2002) Studies on microphysical processes in hail cloud. Chin J Atmos Sci 26:421–432 (in Chinese)

Kistler R, Kalnay E, Collins W, Saha S, White G, Woollen J, Chelliah M, Ebisuzaki W, Kanamitsu M, Kousky V, van den Dool H, Jenne R, Fiorion M (2001) The NCEP-NCAR 50-year reanalysis: monthly means CD-ROM and documentation. Bull Am Meteorol Soc 82:247–268

Klemp JB, Durran DR (1983) An upper boundary condition permitting internal gravity wave radiation in numerical mesoscale models. Mon Wea Rev 111:430–444

Kong FY, Huang MY, Xu HY (1991) Three-dimensional numerical simulations of the effects of ice phase processes on evolution of convective storms. Sci China Ser B 9:1000–1008 (in Chinese)

Li X, Sui C-H, Lau K-M, Chou M-D (1999) Large-scale forcing and cloud-radiation interaction in the tropical deep convective regime. J Atmos Sci 56:3028–3042

Lin WS, Sui C-H, Bueh C, Wang A, Fan S, Wu C, Fong S, Li J, Meng J (2007) Numerical comparison study of cloud microphysical parameterization schemes for a moderate snowfall event in North China. Meteorol Atmos Phys 95:195–204

Molinari J, Dudek M (1992) Parameterization of convective precipitation in mesoscale numerical models: a critical review. Mon Wea Rev 120:326–343

Reisner J, Rasmussen RM, Bruintjes RT (1998) Explicit forecasting of super-cooled liquid water in winter storms using the MM5 mesoscale model. Q J Royal Meterol Soc 124B:1071–1107

Sekhon RS, Srivastiva RC (1970) Snow size spectra and radar reflectivity. J Atmos Sci 27:299–307

Sui C-H, Li X, Lau K-M (1998) Radiative-convective processes in simulated diurnal variations of tropical oceanic convection. J Atmos Sci 55:2345–2357

Tao WK, Simpson J (1993) The Goddard cumulus ensemble model. Part I: model description. Terr Atmos Ocean Sci 4:35–72

Tao WK, Simpson J, Baker D, Braun S, Chou MD, Ferrier B, Johnson D, Khain A, Lans S, Lynn B, Shie CL, Starr D, Sui CH, Wang Y, Wetzel P (2003) Microphysics, radiation and surface processes in the Goddard Cumulus Ensemble (GCE) Model. Meteorol Atmos Phys 82:97–137

Thompson G, Rasmussem RM, Manning K (2004) Explicit forecasts of winter precipitation using an improved bulk microphysical scheme: Part 1: description and sensitivity analysis. Mon Wea Rev 112:519–542

Weisman LM, Skamarock WC, Klemp JB (1997) The resolution dependence of explicitly modeled convective systems. Mon Wea Rev 125:527–548

Woods CP, Stoelinga MT, Locatelli JD (2007) The IMPROVE-1 Storm of 1–2 February 2001. Part III: Sensitivity of a Mesoscale Model Simulation to the Representation of Snow Particle Types and Testing of a Bulk Microphysical Scheme with Snow Habit Prediction. J Atmos Sci 64:3927–3948

Zhang DL (1998) Roles of various diabatic physical processes in mesoscale models. Chin J Atmos Sci 22:548–561 (in Chinese)

Zhang FH (2005) The weather in December 2004. Meteorol Mon 31:90–93 (in Chinese)